A Large Family of Dysprosium-based Trimetallic Nitride Endohedral Fullerenes: Dy$_3$N@C$_{2n}$ (39 ≤ n ≤ 44)

Shangfeng Yang and Lothar Dunsch*

Group of Electrochemistry and Conducting Polymers, Leibniz-Institute for Solid State and Materials Research Dresden, D-01171 Dresden, Germany

Received: March 29, 2005

Dysprosium-based trimetallic nitride endohedral fullerenes (clusterfullerenes)—the Dy$_3$N@C$_{2n}$ (38 ≤ n ≤ 49) family—have been produced at overwhelming yields compared to the empty fullerenes for the first time. The Dy$_3$N@C$_{2n}$ family represents the largest clusterfullerene family explored up to now, even in comparison with the Tm$_3$N@C$_{2n}$ (38 ≤ n ≤ 44) family which was discovered very recently. A series of 10 Dy$_3$N@C$_{2n}$ clusterfullerenes (39 ≤ n ≤ 44, **1**−**9**) have been isolated successfully and characterized by HPLC, mass spectrometry, and UV−vis−NIR spectroscopy. The study on the HPLC elution behavior reveals that there are two isomers for Dy$_3$N@C$_{78}$ and Dy$_3$N@C$_{84}$. Furthermore, a third isomer of Dy$_3$N@C$_{80}$ is isolated for the first time. The optimum production conditions (Dy:C = 1:15, NH$_3$ pressure = 20 mbar) have been determined by investigating the effects of the Dy:C ratio and NH$_3$ pressure on the yields of the Dy$_3$N@C$_{2n}$ clusterfullerenes. UV−vis−NIR spectroscopic study indicates that the Dy$_3$N@C$_{2n}$ clusterfullerenes with small cages (n = 39−41) are large band-gap (1.38∼1.51 eV) materials, while the band-gaps for those with larger cages (n = 42−44) are significantly smaller (0.80∼0.84 eV).

Introduction

Endohedral fullerenes represent a novel type of nanostructures, which are characterized by a robust fullerene cage with atoms, ions, or clusters trapped in its hollow.[1−4] Because of the electron transfer from the encaged species to the fullerene cage, the encapsulation of the encaged species brings about many new properties such as peculiar redox and photoelectrochemical behaviors, luminescence, paramagnetism, and enhanced nonlinear optical response.[1−6] During the past few years the success in preparing macroscopic quantities of endohedral fullerenes has made it possible to isolate a large number of them and characterize their structures and physical properties.[1−14]

Trimetallic nitride endohedral fullerenes (clusterfullerenes), the first novel endohedral fullerenes with a cluster inside, have been attracting the great interest since their discovery by Dorn et al.[15] in 1999 because of the feasibility of tuning the trapped metal atoms and the cage sizes. Trimetallic nitride clusterfullerenes are distinguished by several fascinating properties such as outstanding high yields relative to the empty fullerenes and conventional mono- and dimetallofullerenes, high thermal stability and long-term stability in air.[4,15−18] Among the new clusterfullerene family, Sc$_3$N@C$_{80}$ is the first most abundant member,[15] which can be formally viewed as a positively charged planar cluster of atoms inside a negatively charged icosahedral carbon cage, i.e., [Sc$_3$N]$^{6+}$@C$_{80}$$^{6−}$.[19] Later on, many new clusterfullerenes were produced. For instance, Er$_x$Sc$_{3−x}$N@C$_{80}$ (x = 0−2),[15,20] A$_x$Sc$_{3−x}$N@C$_{68}$ (x = 0−2; A = Tm, Er, Gd, Ho, La) in which the trimetallic nitride is trapped in a non-IPR C$_{68}$ cage,[21] Sc$_3$N@C$_{78}$,[22] Lu$_3$N@C$_{80}$,[23,24] Lu$_{3−x}$A$_x$N@C$_{80}$ (x = 0−2; A = Gd, Ho),[24] Y$_3$N@C$_{80}$,[18] Ho$_3$N@C$_{80}$,[17] and Tb$_3$N@C$_{80}$.[25] Functionalized derivatives of Sc$_3$N@C$_{80}$ were also reported.[26−28] It is noted that, however, most of these known trimetallic nitride clusterfullerenes have been mainly limited to the C$_{80}$ cage.

Very recently, the new clusterfullerene families of Tm$_3$N@C$_{2n}$ (38 ≤ n ≤ 44) and Gd$_3$N@C$_{2n}$ (40 ≤ n ≤ 44) have been successfully produced by our group,[29,30] expanding the family to much higher clusterfullerenes. The Tm$_3$N@C$_{2n}$ family are generally classified to large band-gap (1.2∼1.75 eV) materials.[29] The cage structures of the two isomers of Tm$_3$N@C$_{80}$ are found to be quite similar to those of Sc$_3$N@C$_{80}$, but Tm$_3$N@C$_{78}$ is quite different to Sc$_3$N@C$_{78}$,[29,31] suggesting that the structure of the trimetallic nitride clusterfullerene is quite dependent on the metal element. For the Gd$_3$N@C$_{2n}$ family where Gd$_3$N is the largest cluster encaged in fullerene cages to date, however, a relatively lower abundance of Gd$_3$N@C$_{80}$ (I) in comparison with Sc$_3$N@C$_{80}$ (I) and Tm$_3$N@C$_{80}$ (I) was revealed; this was understood by considering two important factors including the larger metal ion radius for Gd and the weaker metal-nitrogen bond strength for Gd$_3$N clusterfullerenes.[30] Moreover, the dependence of the abundance and stability of the clusterfullerenes on the trimetallic nitride cluster composition has been demonstrated based on the systematic comparison for M$_3$N@C$_{80}$ (M = Er, Y, Ho, Tb).[4] It is then reasonable to question whether other metal elements could form such clusterfullerene structures and whether the clusterfullerenes with cages even larger than C$_{88}$ could be produced.

On the other hand, it has already been known that there are two isomers of M$_3$N@C$_{80}$ (M = Sc, Tm) that had been isolated, and they show quite different cage and electronic properties.[29,31,32] Since theoretical study indicates that there are seven isomers for a C$_{80}$ cage obeying the isolated pentagon rule (IPR),[33] an intriguing question is raised whether there exist other isomeric forms for this cage. Likewise, the same question should be addressed for other clusterfullerenes with different fullerene cages.

* Corresponding author. E-mail: l.dunsch@ifw-dresden.de.

Dy$_3$N@C$_{2n}$ Endohedral Fullerenes

*J. Phys. Chem. B, Vol. 109, No. 25, 2005* **12321**

In this paper, we report the production, isolation, and spectroscopic characterization of a new large family of clusterfullerenes based on dysprosium—the Dy$_3$N@C$_{2n}$ ($39 \leq n \leq 44$)—for the first time. Dysprosium (Dy) is investigated since the properties of the conventional Dy-based metallofullerenes Dy$_m$@C$_{2n}$ have been comprehensively studied and this would provide good comparison basis.[3,6,12–14,34] Another noteworthy point is that the radius of Dy^{3+} (0.91 Å) is larger than Sc^{3+} (0.75 Å) and Tm^{3+} (0.87 Å) while comparable to Gd^{3+} (0.94 Å).[30,35] It would be quite interesting to investigate whether the Dy-based clusterfullerenes could be produced and whether they would exhibit a relatively low yield like the Gd$_3$N@C$_{2n}$ clusterfullerenes.[30] High-performance liquid chromatography (HPLC) and laser desorption time-of-flight (LD-TOF) mass spectrometry (MS) were used to isolate and identify the Dy$_3$N@C$_{2n}$ clusterfullerenes. The effects of the Dy:C ratio and NH$_3$ pressure on the yields of the clusterfullerenes were studied and the optimum production conditions were consequently determined. Electronic properties and band-gaps of the Dy$_3$N@C$_{2n}$ clusterfullerenes were investigated by UV−vis−NIR spectroscopy.

Experimental Section

General procedures for the production of clusterfullerenes by a modified Krätschmer-Huffman DC-arc discharging method have been described elsewhere.[4,16,17,29–31] A mixture of dysprosium oxide (Dy$_2$O$_3$, 99.9%, MaTeck GmbH, Germany) and graphite powder was pressed into the hole of graphite rod electrode (ϕ 4.5 mm) in a certain Dy:C molar ratio, which was variable from 1:10 to 1:50 (typically 1:15), to study the effect of the mixing ratio on the yield of the clusterfullerenes. As the source of nitrogen, NH$_3$ was introduced into the reactor atmosphere of 200 mbar He at a certain pressure, which varied from 10 to 40 mbar (typically 20 mbar), to investigate its influence on the yield of clusterfullerenes. After DC-arc discharging, the soot was collected under ambient conditions and first pre-extracted with acetone for several hours to remove the nonfullerene hydrocarbon byproducts. The as purified soot was then Soxhlet extracted by CS$_2$ for 20 h. The resulting brown-yellow solution was distilled to remove CS$_2$, and the mixture powder was immediately redissolved in toluene (∼10 mL) and subsequently passed through a 0.2 μm Teflon filter (Sartorius AG, Germany) for HPLC separation.

Clusterfullerene separation was performed by multi-stage HPLC running in a Hewlett-Packard instrument (series 1050), with toluene used as the eluent (mobile phase). In the first stage, the mixture was separated into eight fractions (see Figure 1-I) using a linear combination of two analytical 4.6 × 250 mm Buckyprep columns (Nacalai Tesque, Japan), a flow rate of 1.6 mL/min, and an injection volume of 500 μL. Further separations of the two mixture fractions (**3+3′, 4+5**) were accomplished by an additional stage on a semipreparative 10 × 250 mm Buckyclutcher column (Regis, USA) applying a flow rate of 1.0 mL/min and an injection volume of 250 μL. An ultraviolet detector set to 320 nm was used for fullerene detection. The purity of the isolated fractions was checked by HPLC runs which were performed on both Buckyprep and Buckyclutcher columns, followed by LD-TOF MS analysis running in both positive and negative ion modes (Biflex III, Bruker, Germany).

UV−vis−NIR spectra of the clusterfullerenes dissolved in toluene were recorded on a UV−vis−NIR 3101-PC spectrometer (Shimadzu, Japan) using quartz cell of 1 mm layer thickness and 1 nm resolution.
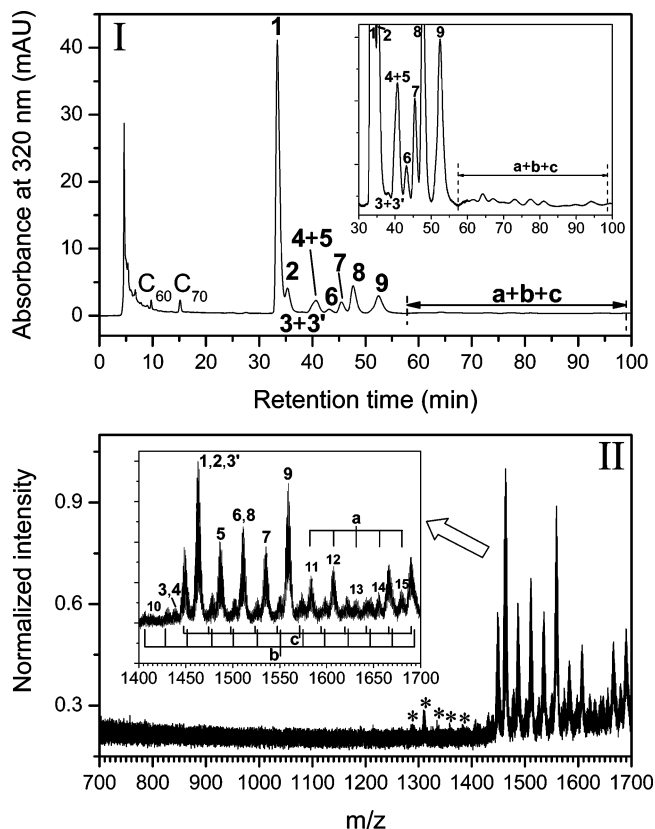
Figure 1. (I) Chromatogram of a Dy$_3$N@C$_{2n}$ fullerene extract (linear combination of two 4.6 × 250 mm Buckyprep columns; flow rate 1.6 mL/min; injection volume 500 μL; toluene as eluent; 40 °C). The peak around 5 min is due to the hydrocarbon byproducts. The inset shows the enlarged region without the empty fullerenes. (II) Positive ion LD-TOF mass spectrum of the fullerene extract. The asterisks represent dimetallofullerenes (Dy$_2$@C$_{2n}$, $40 \leq n \leq 44$). The inset is the enlarged region showing the intense mass peaks: (a) clusterfullerenes (Dy$_3$N@C$_{2n}$, $45 \leq n \leq 49$); (b) dimetallofullerenes (Dy$_2$@C$_{2n}$, $45 \leq n \leq 57$); (c) trimetallofullerenes (Dy$_3$@C$_{2n}$, $40 \leq n \leq 50$).

Results and Discussion

Identification of the Dy$_3$N@C$_{2n}$ Clusterfullerenes. As demonstrated previously, by using NH$_3$ as the reactive gas atmosphere, the selectivity of the clusterfullerene structure production in the fullerene soot extract is significantly enhanced up to 90% of a total amount in the mg range.[4] Similarly, the production of the Dy$_3$N@C$_{2n}$ clusterfullerenes also exhibits such a pronounced enhancement while the clusterfullerene members are even more enlarged. Shown in Figure 1-I is the typical chromatogram for a fullerene extract obtained under the optimum production conditions (Dy:C = 1:15, NH$_3$ pressure = 20 mbar). The relative yields of the 10 separable fractions (products) which are produced with considerably high abundances reach up to 98% of all of the fullerenes, overwhelmingly higher than those of the empty fullerenes (∼2%). This is similar to the Sc$_3$N@C$_{2n}$ and Tm$_3$N@C$_{2n}$ families but apparently contrary to the case of the Gd$_3$N@C$_{2n}$ clusterfullerenes, where the yield of Gd$_3$N@C$_{80}$ (I) is quite low, and comparable to the empty fullerenes C$_{60}$ and C$_{70}$.[29–31] The difference in the strength of the metal−nitrogen bond in the trimetallic nitride cluster could account partly for the great differences on the abundances of these clusterfullerenes.[30]

Furthermore, the mass spectrum (MS) of the extract shown in Figure 1-II gives the direct evidence for the formation of the Dy$_3$N@C$_{2n}$ clusterfullerenes with cages ranging from C$_{76}$ (n = 38) to C$_{98}$ (n = 49). Such a family is much larger than all of

12322 *J. Phys. Chem. B, Vol. 109, No. 25, 2005*

Yang and Dunsch

TABLE 1: Characteristics of the $Dy_3N@C_{2n}$ Clusterfullerenes Produced in This Work

no.	n	product	retention time (min)		mass number (m/z)
			Buckyprep[a]	Buckyclutcher[b]	
1	40	$Dy_3N@C_{80}$ (I)	33.4	22.0	1461.5
2	40	$Dy_3N@C_{80}$ (II)	35.3	22.0	1461.5
3	39	$Dy_3N@C_{78}$ (I)	38.2	22.1	1437.5
3′	40	$Dy_3N@C_{80}$ (III)	38.2	25.7	1461.5
4	39	$Dy_3N@C_{78}$ (II)	40.7	22.0	1437.5
5	41	$Dy_3N@C_{82}$	40.7	23.2	1485.5
6	42	$Dy_3N@C_{84}$ (I)	43.1	23.3	1509.5
7	43	$Dy_3N@C_{86}$	45.4	23.9	1533.5
8	42	$Dy_3N@C_{84}$ (II)	47.6	24.2	1509.5
9	44	$Dy_3N@C_{88}$	52.4	24.8	1557.5
10	38	$Dy_3N@C_{76}$	$-^c$	$-^c$	1413.5
11	45	$Dy_3N@C_{90}$	$-^c$	$-^c$	1581.5
12	46	$Dy_3N@C_{92}$	61.6	29.9	1605.5
13	47	$Dy_3N@C_{94}$	$-^c$	$-^c$	1629.5
14	48	$Dy_3N@C_{96}$	$-^c$	$-^c$	1653.5
15	49	$Dy_3N@C_{98}$	$-^c$	$-^c$	1677.5

[a] Linear combination of two Buckyprep columns. Flow rate of toluene: 1.6 mL/min. [b] Flow rate of toluene: 1.0 mL/min. See Supporting Information. [c] These data are to be confirmed yet due to the extremely low yields of the products.

the other $M_3N@C_{2n}$ (M = Sc, Y, Gd, Tb, Ho, Er, Tm, Lu) clusterfullerene families reported to date.[15−25,29−31] The assignments of the detected mass peaks are summarized in Table 1 together with the HPLC retention times of the products. Among the large $Dy_3N@C_{2n}$ family, clusterfullerenes with cages between C_{78} and C_{88} ($39 \leq n \leq 44$, **1−9**) are produced at distinguishingly high yields and have conventional fullerene cage sizes which are believed crucial for their stabilities. These clusterfullerenes are thus focused for further isolation and characterization. In addition, five $Dy_3N@C_{2n}$ clusterfullerenes with cages higher than C_{88} (fraction a, $45 \leq n \leq 49$, **11−15**) are also produced and exhibit quite large retention times (see insets), being the largest clusterfullerenes discovered to date but not subjected to isolation due to their extremely low yields as indicated in the chromatogram and their unknown low stabilities. On the other hand, like the $Sc_3N@C_{2n}$ and $Tm_3N@C_{2n}$ families,[22,29,31] the $Dy_3N@C_{2n}$ clusterfullerenes with cages smaller than C_{80}, such as C_{76} (**10**) and C_{78} (**3, 4**), are also detected. This is, however, remarkably different to the case of the $Gd_3N@C_{2n}$ clusterfullerenes again, where C_{80} is regarded as the size threshold for the encapsulation of the Gd_3N cluster in fullerene cages due to the cluster size constraint.[30] As a matter of fact, using the common way in the literature to estimate the diameter of the M_3N cluster ($d(M_3N) \propto 4r(M^{3+})$, where r is the radius of the metal ion),[30,35] one may find that the Dy_3N cluster ($r(Dy^{3+}) = 0.91$ Å) is only ∼ 0.12 Å smaller than Gd_3N ($r(Gd^{3+}) = 0.94$ Å) in diameter. With only such a small decrease from Gd_3N to Dy_3N, the cluster size constraint is dramatically broken.[30] Nevertheless, the close resemblance of the $Dy_3N@C_{2n}$ clusterfullerenes to $Sc_3N@C_{2n}$ and $Tm_3N@C_{2n}$ is largely attained, regardless of the fact that the Dy_3N cluster is larger than Sc_3N ($r(Sc^{3+}) = 0.75$ Å) and Tm_3N ($r(Tm^{3+}) = 0.87$ Å).[35] Since the same type and strength of cluster-cage interaction has been revealed for different $M_3N@C_{80}$ (M = Sc, Y, Gd, Tb, Ho, Er, Tm) clusterfullerenes,[30] it appears that the cluster-cage interaction plays a less important role on the cage size distribution and abundance of these clusterfullerenes than the cluster size.

A further check for the relative yield of the $Dy_3N@C_{2n}$ clusterfullerens to the empty fullerene C_{60} indicates that, except **3**, **3′**, and **6**, the other clusterfullerenes are produced at even higher yields than C_{60} (see Figure 1-I). Such a feature was not

demonstrated for the cases of the $Sc_3N@C_{2n}$ and $Tm_3N@C_{2n}$ clusterfullerenes, where only the yields of the main products $M_3N@C_{80}$ (I and II) exceeded C_{60}.[29,31] In this sense, the $Dy_3N@C_{2n}$ clusterfullerenes appear quite unique because of the feasibility of producing the higher clusterfullerenes with the fullerene cages larger than C_{80} at high yields. However, it should be noted that the relative yield study should be based on the chromatogram mainly instead of the MS, because the intensity of the mass peak depends strongly on the ionization mode under LD-TOF MS condition. Under positive ion mode, the empty fullerenes are much more difficult to be ionized than the clusterfullerenes, so the mass peaks of the empty fullerenes such as C_{60} and C_{70} are even not detected at all in Figure 1-II although the chromatogram clearly indicates their formations. On the contrary, they tend to exhibit exaggerated intensities under negative ion mode where ionizations of the clusterfullerenes become more difficult.

In addition to the favorable production of the $Dy_3N@C_{2n}$ clusterfullerenes, another remarkable feature of the present method is that the addition of NH_3 is found to benefit also the production of a large series of dimetallofullerenes ($Dy_2@C_{2n}$, $40 \leq n \leq 57$) and even trimetallofullerenes (fraction c, $Dy_3@C_{2n}$, $40 \leq n \leq 50$) as the byproducts, with the yields being even higher than those of the mono-metallofullerenes (see the inset of Figure 1-II). As a result, the detected dimetallofullerene family is much larger than the reported series of Dy-based metallofullerenes which were isolated by recycling HPLC,[34] suggesting the feasibility of producing the dimetallofullerenes with new larger fullerene cages and the prospect of isolating them by single-stage HPLC, since dimetallofullerenes such as $Dy_2@C_{94}$ (I, II) and $Dy_2@C_{100}$ have been isolated.[36a] This feature had never been achieved by the conventional arc discharging method without NH_3 added, by which the production of the empty fullerenes and mono-metallofullerenes are dominant instead.[1−3] It is thus reasonable to consider that the beneficial effect is accomplished by suppressing the production of the empty fullerenes and mono-metallofullerenes, as will be discussed in the later part.

In the fullerene extract, **1** ($Dy_3N@C_{80}$ (I)) is the most abundant product. This is no wonder since the previous studies on $Sc_3N@C_{2n}$ and $Tm_3N@C_{2n}$ have already revealed the unusually high yield for $M_3N@C_{80}$.[29,31] Excluding **2** ($Dy_3N@C_{80}$ (II)), the relative yield of **1** reaches up to 65−70% of all of the fullerenes; this is similar to the cases of the other $M_3N@C_{2n}$ clusterfullerenes (M = Sc, Y, Tb, Ho, Er, Tm) clusterfullerenes but much higher than that of $Gd_3N@C_{2n}$ clusterfullerenes.[4,29−31] The relative abundance of the second isomer (**2**) in the entire $Dy_3N@C_{80}$ fraction is approximately 10%, comparable to that for $Gd_3N@C_{80}$ (II), while only half as high as for $Sc_3N@C_{80}$ (II) and $Tm_3N@C_{80}$ (II).[29−31] A noteworthy difference between **2** and other $M_3N@C_{80}$ (II) (M = Sc, Tm) is that its relative yield is even lower than the other two higher clusterfullerenes, **8** ($Dy_3N@C_{84}$ (II)) and **9** ($Dy_3N@C_{88}$). Such an unusual abundance distribution was also observed for the $Gd_3N@C_{2n}$ clusterfullerenes,[30] suggesting the preferential formation of the higher clusterfullerenes for large clusters. Moreover, it is generally found that the relative abundance of those $Dy_3N@C_{2n}$ higher clusterfullerenes ($n = 41−44$) are higher than that in the $Tm_3N@C_{2n}$ clusterfullerene family.[29] Therefore, these results indicate that the Dy_3N cluster is quite flexible to be encapsulated into the fullerene cage with the largest variability.

Isolation of the Abundant $Dy_3N@C_{2n}$ Clusterfullerenes ($39 \leq n \leq 44$, 1−9). Like the conventional endohedral fullerenes, the $Dy_3N@C_{2n}$ clusterfullerenes **1−9** are quite stable

Dy$_3$N@C$_{2n}$ Endohedral Fullerenes

J. Phys. Chem. B, Vol. 109, No. 25, 2005 **12323**
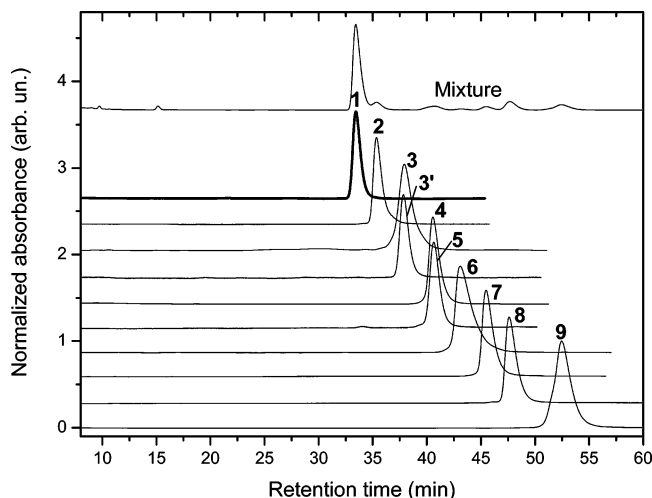
Figure 2. Chromatograms of the isolated products **1**−**9** and the extract mixture (linear combination of two 4.6 × 250 mm Buckyprep columns; flow rate 1.6 mL/min; injection volume 100 μL; toluene as eluent (mobile phase); 40 °C). The chromatogram of the mixture is copied from Figure 1-I.
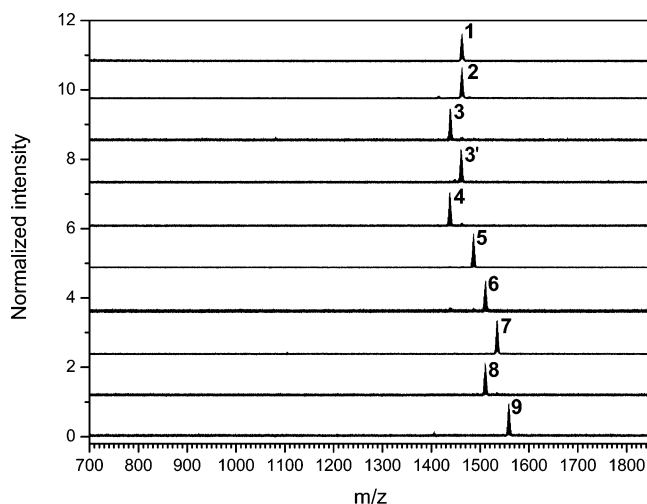
Figure 3. Positive ion laser desorption time-of-flight (LD-TOF) mass spectra (MS) of the isolated products **1**−**9**.

throughout the chromatographic separation process and under LD-TOF MS measurement conditions. This feature leads us to accomplish effective isolation of them. Chemical identities and purities of the isolated Dy$_3$N@C$_{2n}$ clusterfullerenes **1**−**9** are established by the chromatograms and MS shown in Figures 2 and 3, respectively, indicating a considerably high purity for all of the products. In addition, Figure 4 provides a closer comparison of the measured isotope distributions for all of the 10 products with the theoretical calculations. In all cases the good agreement is obtained, confirming the chemical identities as listed in Table 1. It should be noted that, as already revealed in Figure 1-I, **3** and **3′** exist in the form of mixture and exhibit nearly same retention times when the Buckyprep column is used in the first stage. Hence, an additional separation on the Buckyclutcher column is necessary for an effective isolation. The same case also happens for **4** and **5**. Nevertheless, the other products are simply isolated by the single-stage HPLC separation on Buckyprep column. Moreover, further purity tests of the products are additionally carried out by HPLC runs performed on a Buckyclutcher column to verify whether there is a similar coexistence of any other product as impurity. The purity of the product could then be determined based on both of the HPLC runs and MS analysis, and the results are listed in Table 2. In

addition to the two isomers of Dy$_3$N@C$_{80}$ (**1,2**), the purity of all other higher clusterfullerenes Dy$_3$N@C$_{2n}$ (**5**−**9**, $n = 41$−44) is ≥95% and the amounts reach up to the mg range too. Such a successful isolation by single-stage HPLC for most products has never been realized for the other M$_3$N@C$_{2n}$ (M = Sc, Tm, Gd) clusterfullerenes.[29−31] We believe that this is attributable to both the high yields of the Dy$_3$N@C$_{2n}$ clusterfullerenes and the judicious choices of the production and separation conditions.

An interesting finding is that there are isomers for several Dy$_3$N@C$_{2n}$ clusterfullerenes, namely, Dy$_3$N@C$_{78}$ (**3**, **4**), Dy$_3$N@C$_{80}$ (**1**, **2**, **3′**), and Dy$_3$N@C$_{84}$ (**6**, **8**). For Dy$_3$N@C$_{80}$, in addition to the two isomers (**1**, **2**) that were also reported for other M$_3$N@C$_{80}$ (M = Sc, Tm, Gd),[29−32] a third isomer (**3′**) is isolated for the first time, exhibiting the same retention time as **3** on the Buckyprep column (see Figures 1-I and 2) but much longer retention time (25.7 min) than **1**−**3** (22.0−22.1 min) on the Buckyclutcher column. The fact that the retention times of **3′** on both Buckyprep and Buckyclutcher columns are much larger than **1** and **2** suggests that the dipole and/or quadrupole moments of **3′**, which are caused by the nonspherical charge distribution due to the elongated elliptical cage, are larger.[37] A similar explanation was proposed for understanding the retention behavior of Tm$_3$N@C$_{78}$.[29] The identification and detailed analysis of **3′** will be reported elsewhere.[36b]

On the other hand, two isomers for Dy$_3$N@C$_{78}$ and Dy$_3$N@C$_{84}$ are successfully isolated too, which had not been found before for other M$_3$N@C$_{2n}$ (M = Sc, Tm, Gd) clusterfullerene families.[29−31] The discoveries of these isomers is easily understood because 5 and 24 IPR-satisfying isomers are expected for C$_{78}$ and C$_{84}$ cages respectively according to the theoretical study.[33] To our surprise, however, **4** (Dy$_3$N@C$_{78}$ (II)) exhibits the same retention time as **5** (Dy$_3$N@C$_{82}$), while the retention time of **8** (Dy$_3$N@C$_{84}$ (II)) is even larger than that of its neighboring higher clusterfullerene **7** (Dy$_3$N@C$_{86}$) on the Buckyprep column. The more intriguing point is that the second isomers for Dy$_3$N@C$_{78}$ and Dy$_3$N@C$_{84}$ (**4**, **8**) are even more abundant than the first ones (**3**, **6**) and become the "major" isomers, violating the general definition for distinguishing "major" and "minor" isomers completely.[1,38] Because of the interferences of these isomers, the elution behavior and relative abundance of the Dy$_3$N@C$_{2n}$ clusterfullerenes **1**−**9** are totally different from the cases of the other M$_3$N@C$_{2n}$ (M = Sc, Tm, Gd) clusterfullerene families where only isomers for M$_3$N@C$_{80}$ had been isolated.[29−32] A probable explanation is that the isomers for M$_3$N@C$_{78}$ and M$_3$N@C$_{84}$ (M = Sc, Tm, Gd), even if exist, would be negligible and much more difficult to be detected due to their much lower yields. Anyway, such a distinct difference further illustrates the uniqueness of the present Dy$_3$N@C$_{2n}$ clusterfullerene family and the strong influence of the metal element on the nitride clusterfullerene formation.[4,30] Additionally, by comparing the Dy$_3$N@C$_{2n}$ clusterfullerenes with the counterparts (same fullerene cages) of the other reported M$_3$N@C$_{2n}$ (M = Sc, Tm, Gd) clusterfullerenes, one may note that the retention times of all of the Dy$_3$N@C$_{2n}$ clusterfullerenes **1**−**9** are generally smaller under the same separation conditions (two Buckyprep columns and flow rate of 1.6 mL/min).[29−31] Such a time shift is believed due to the different isolation performances obtained by the two different HPLC instruments that we used.

Effects of the Dy:C Ratio and NH$_3$ Pressure on the Production Selectivity of the Dy$_3$N@C$_{2n}$ Clusterfullerenes. To optimize the production condition so as to produce the Dy$_3$N@C$_{2n}$ clusterfullerenes at high yields, we study the effects
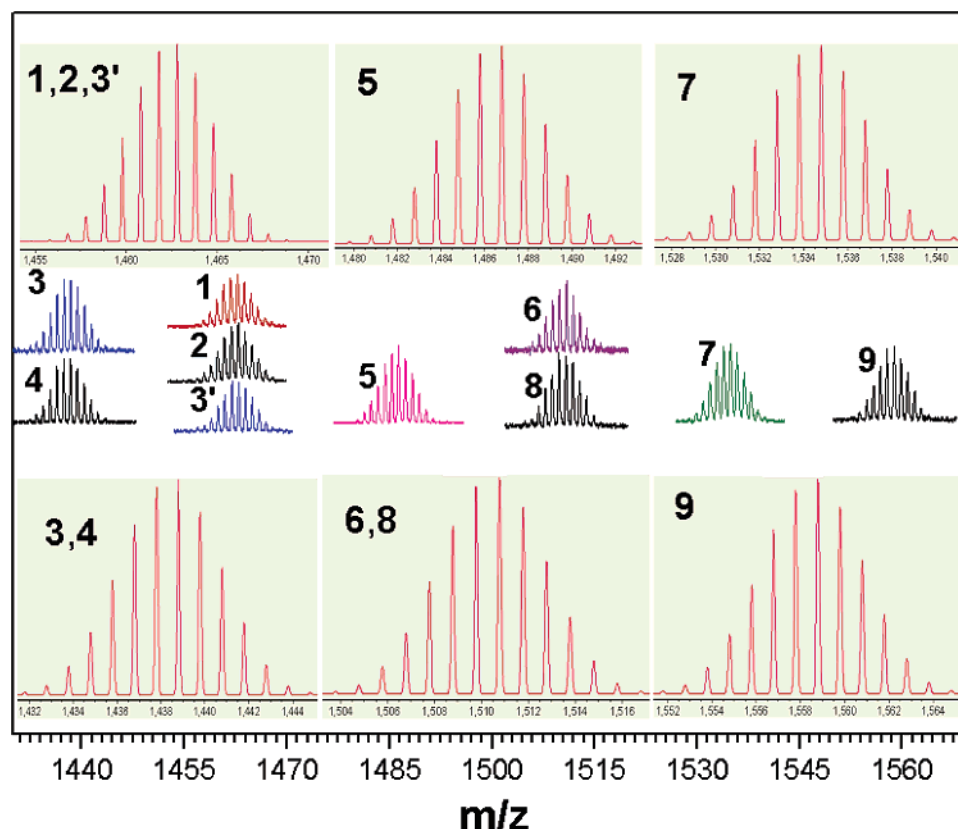
Figure 4. Measured and calculated isotope distributions of the isolated products **1–9**. The measured isotope distributions are based on Figure 3.

TABLE 2: Characteristics Electronic Absorption Properties of the Isolated $Dy_3N@C_{2n}$ Clusterfullerenes

| no.	n	product	onset (nm)	band-gap[a] (eV)	UV−vis−NIR absorption peaks (nm)	purity[b] (%)	color of the toluene solution[c]
1	40	$Dy_3N@C_{80}$ (I)	823	1.51	320, 401, 554, 626, 643, 670, 700	≥99	orange
2	40	$Dy_3N@C_{80}$ (II)	929	1.33	463, 627, 714	≥98	dark yellow
3	39	$Dy_3N@C_{78}$ (I)	917	1.35	394, 748	≥90	light yellow
4	39	$Dy_3N@C_{78}$ (II)	933	1.33	402, 553, 598, 670, 741	≥99	brown
5	41	$Dy_3N@C_{82}$	900	1.38	387, 436, 505, 625	≥98	brown-red
6	42	$Dy_3N@C_{84}$ (I)	1514	0.82	622, 870	≥95	yellow
7	43	$Dy_3N@C_{86}$	1482	0.84	326, 448, 642	≥99	green
8	42	$Dy_3N@C_{84}$ (II)	1485	0.84	374, 484, 625	≥99	green-yellow
9	44	$Dy_3N@C_{88}$	1548	0.80	345, 733, 1045, 1462	≥96	brown-yellow

[a] The band-gap is calculated from the spectral onset (bandgap (eV) ≈ 1240/onset (nm)). See Supporting Information. [b] Based on the integration results of the chromatograms running on both Buckyprep and Buckyclutcher columns and LD-TOF mass spectra running in positive-ion mode. [c] Because of the effect of the sunlight, the colors of **3** and **6** shown in Figure 10 are not evident due to their relatively low concentrations.

of the Dy:C ratio and NH_3 pressure. Figure 5 presents the chromatograms of a series of fullerene extracts obtained under different Dy:C molar ratios ranging from 1:10 to 1:50 but constant He (200 mbar) and NH_3 (20 mbar) pressures, indicating the strong dependence of the yields of not only the $Dy_3N@C_{2n}$ clusterfullerenes but also of the empty fullerenes (mainly C_{60} and C_{70}) on the Dy:C ratio. Since the relative yields of **2–9** to the most abundant product **1** keep constant with the change of the Dy:C ratio, **1** is chosen as the representative to simplify the analysis. The influence of the C:Dy (or Dy:C) ratio on the yield of **1**, which is correlated to the HPLC peak intensity, is plotted in Figure 6 (curve a) where the relative yield of **1** to C_{60} (retention time: 9.6 min) is also included (curve b). At a relatively high Dy:C (or low C:Dy) molar ratio from 1:30 to 1:10, the production of **1** appears to be much more dominant than C_{60}, indicating that a relatively high Dy:C ratio is favorable for the formation of the $Dy_3N@C_{2n}$ clusterfullerene instead of C_{60}. The yield of **1** increases slowly with the increase of Dy:C ratio (decrease of C:Dy) at first and reaches the maximum at the optimum ratio of 1:15, while the further increase results in

the sharp decrease of the yield instead. The relative yield of **1** to C_{60} follows the same trend, except for the sharper increase and also it exhibits the maximum (∼25) at the ratio of 1:15. When the Dy:C ratio is as low as 1:40, on the contrary, the yield of C_{60} becomes comparable to that of **1** and the productions of **1** and C_{60} are balanced. The further decrease of the ratio to 1:50, however, results in an extreme break of such a balance due to the strong suppression of the formation of **1**. In this case, the production of the empty fullerenes becomes dominant while clusterfullerenes are in turn negligible.

As proposed previously, it is believed that the addition of NH_3 would give rise to the chemical reaction between the metal (oxide) and NH_3, resulting in the formation of a trimetallic cluster structure which is only stable as an endohedral cluster in a carbon cage.[4] Thus we can interpret the great influence of the Dy:C ratio discussed above. Since all of the above-mentioned fullerene extracts are obtained under the constant NH_3 pressure condition (20 mbar), it is reasonable to expect that changing the Dy:C ratio, which correlates to the relative amount of Dy_2O_3, would influence the reaction.[4] It is then necessary to investigate
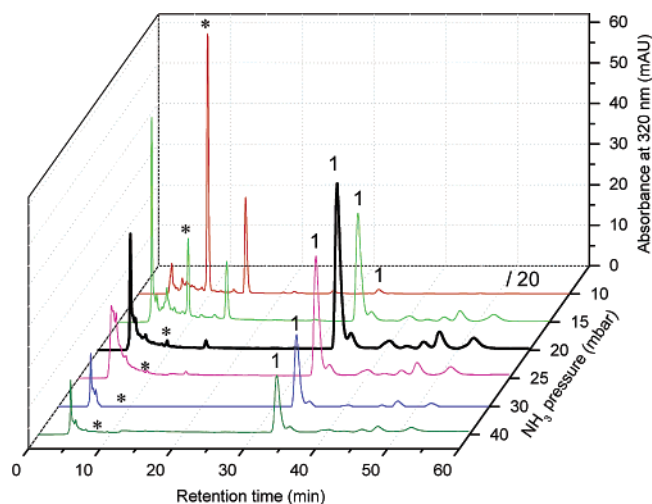
Dy₃N@C₂n Endohedral Fullerenes

J. Phys. Chem. B, Vol. 109, No. 25, 2005 **12325**
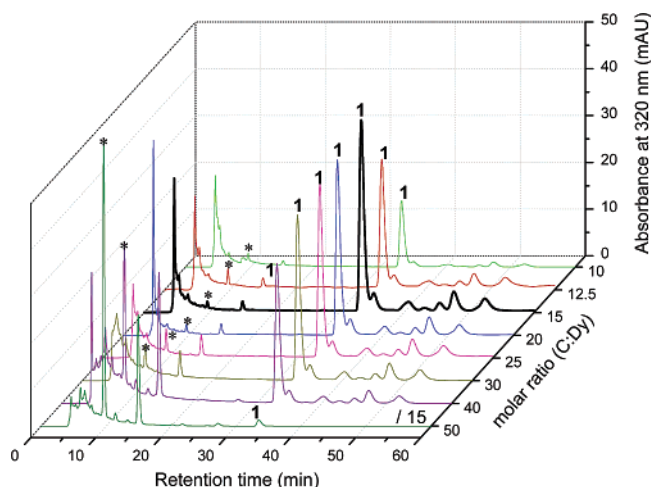
Figure 5. Chromatogram of the $Dy_3N@C_{2n}$ fullerene extracts obtained under different Dy:C ratio (linear combination of two 4.6×250 mm Buckyprep columns; flow rate 1.6 mL/min; injection volume 100 μL; toluene as eluent (mobile phase); 40 °C). The asterisks represent C_{60}.
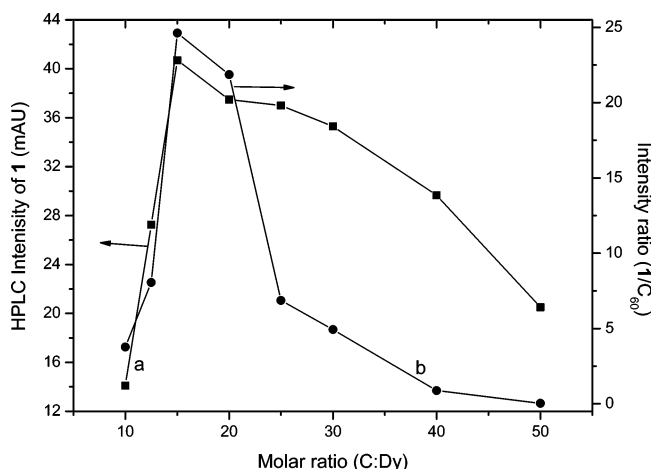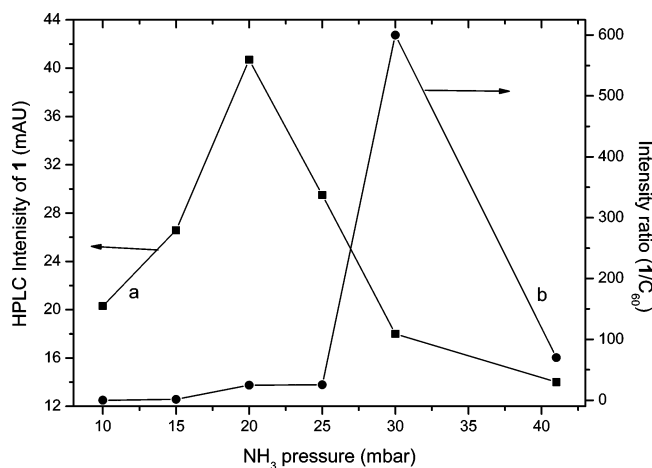

Figure 6. Effect of the Dy:C ratio on the yield of **1** (curve a) and relative yield of **1** to C_{60} (curve b).

Figure 7. Chromatogram of the $Dy_3N@C_{2n}$ fullerene extracts obtained under different NH_3 pressure (linear combination of two 4.6×250 mm Buckyprep columns; flow rate 1.6 mL/min; injection volume 100 μL; toluene as eluent (mobile phase); 40 °C). The asterisks represent C_{60}.

Figure 8. Effect of NH_3 pressure on the yield of **1** (curve a) and relative yield of **1** to C_{60} (curve b).

the influence of NH_3 on the formations of the $Dy_3N@C_{2n}$ clusterfullerenes. Different fullerene extracts are produced under identical conditions (Dy:C = 1:15, He pressure = 200 mbar) but different NH_3 pressure. The chromatograms are shown in Figure 7, indicating that the yields of both the clusterfullerenes and the empty fullerenes are very sensitive to NH_3 pressure. In the same way as above, the yield of **1** and the relative yield of **1** to C_{60} upon changing NH_3 pressure are plotted in Figure 8. The yield of **1** increases sharply with the increase of NH_3 pressure at first and reaches the maximum at the optimum pressure of 20 mbar, confirming that the relatively high NH_3 amount (pressure) is crucial for the formation of the $Dy_3N@C_{2n}$ clusterfullerens, while the further increase of the NH_3 pressure results in a sharp decrease of the yield instead (curve a). This effect is identical to the influence of the Dy:C ratio discussed above, revealing that both Dy_2O_3 (Dy:C ratio) and NH_3 play important roles to govern the clusterfullerene formation. The optimum conditions (Dy:C = 1:15, NH_3 pressure = 20 mbar) are then understood as a result of the equilibrium of the chemical reaction between Dy_2O_3 and NH_3.[4] When the amount of either Dy_2O_3 (Dy:C ratio) or NH_3 is too low or high, such an equilibrium would be shifted, resulting in a negative effect— decrease of the yields of the clusterfullerenes. Furthermore, when NH_3 pressure exceeds 30 mbar, the production of the empty fullerenes C_{60} is surprisingly suppressed almost completely and

the relative yield of **1** to C_{60} reaches up to 600 (curve b), although the yield of **1** is actually lower than that obtained under 20 mbar NH_3. In this case, the continuous increase of the relative yield of **1** to C_{60} suggests a strong suppression effect of the excessive NH_3 on the formation of empty fullerenes. Although this is not fully understood at present due to the paucity of the knowledge on fullerene formation mechanism, a plausible interpretation could be proposed that the excessive NH_3 might react with carbon atom in the gas phase easily and consequently suppress the process of empty fullerene cage formation because of the formation of hydrocarbons.[4] In this way, the beneficial effect for di- and trimetallofullerenes discussed before could be understood because the increase on the formation probabilities of these metallofullerenes is expected upon such a suppression effect.

To conclude, these results confirm that the chemical reaction between Dy_2O_3 and NH_3 would take place prior to fullerene cage formation.[4] The optimum conditions for the production of the $Dy_3N@C_{2n}$ clusterfullerenes at relatively high yields are determined (Dy:C = 1:15 and NH_3 pressure = 20 mbar), which are interpreted in terms of the equilibrium of the chemical reaction. It is the application of such optimum discharging conditions that enables us to separate the whole large family of

12326 *J. Phys. Chem. B, Vol. 109, No. 25, 2005*

Yang and Dunsch
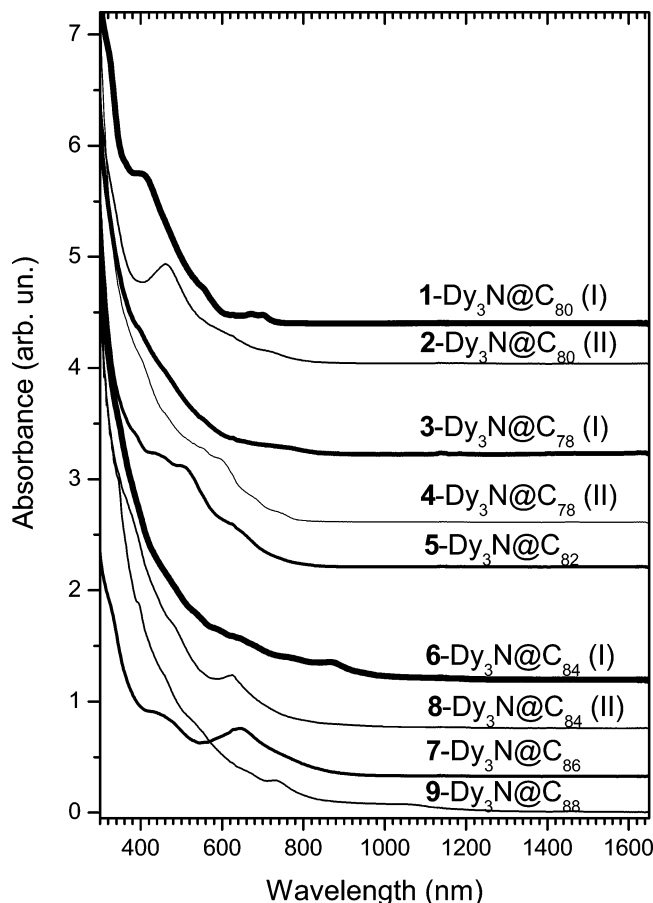
Figure 9. UV−vis-NIR spectra of the $Dy_3N@C_{2n}$ clusterfullerenes **1**−**9** dissolved in toluene.

$Dy_3N@C_{2n}$ clusterfullerenes, including those several isomers which are produced at very low yields.

Electronic Absorption Spectra of the Isolated $Dy_3N@C_{2n}$ Clusterfullerenes 1−9. Presented in Figure 9 are UV−vis−NIR spectra of the isolated $Dy_3N@C_{2n}$ clusterfullerenes **1**-**9** dissolved in toluene. The characteristic spectral onsets and absorption peaks are listed in Table 2. First, the optical band-gap could be estimated according to the onset of the electronic absorption spectrum,[1,15,34,39] the data are also included in Table 2 for comparison. Interestingly, the band-gap of the $Dy_3N@C_{2n}$ clusterfullerenes could be classified to two ranges, i.e., 1.38 eV (**5**) ∼ 1.51 eV (**1**) (for n = 39−41) and 0.80 eV (**9**) ∼ 0.84 eV (**7**, **8**) (for n = 42−44), depending on the fullerene cage. Using the borderline of 1.0 eV to distinguish large and small band-gap fullerenes,[29] we may point out that the $Dy_3N@C_{2n}$ clusterfullerenes with small cages (n = 39−41) are large band-gap (1.38 ∼ 1.51 eV) materials while the band-gaps for those with larger cages (n = 42−44) are significantly smaller (0.80 ∼ 0.84 eV). Furthermore, the spectra of the $Dy_3N@C_{2n}$ clusterfullerenes are also compared with the other corresponding $M_3N@C_{2n}$ (M = Sc, Tm, Gd) clusterfullerenes and $M_2@C_{2n}$ (M = Sc, La, Dy, Er, Tm, n = 39−44) dimetallofullerenes counterparts.[29−31,39−43] Different than the $Tm_3N@C_{2n}$ clusterfullerenes, the correlation of the band-gap ordering with the abundance of clusterfullerenes in the fullerene extract is not applicable for the present $Dy_3N@C_{2n}$ clusterfullerenes.[29]

It is known that the electronic absorptions are predominantly due to π−π* carbon cage transitions and depend on the structure and charge state of the carbon cage.[1,4] For **1**, the spectral onset (∼823 nm), HOMO−LUMO transition peaks (670, 700 nm) and strongest visible absorption peak (401 nm) are all quite close

to the other $M_3N@C_{80}$ (I) (M = Sc, Tb, Ho, Y, Er, Tm, Gd) counterparts,[4,29−31] implying their identities in the cage and electronic structures. The spectrum of **2**, exhibiting the onset of ∼929 nm, is found to be also very similar to those of $Sc_3N@C_{80}$ (II) and $Tm_3N@C_{80}$ (II).[29,31]

It is found that **4** gives a very close absorption spectrum to that of $Tm_3N@C_{78}$,[29] suggesting the similarities of the cage structures. However, both spectra are significantly different to that of $Sc_3N@C_{78}$ as discussed previously,[29,31] indicating the distinct discrepancy in their cage structures. On the other hand, as the first isomer of $Dy_3N@C_{78}$ with a lower abundance than the second one, clearly **3** is additionally distinguished from **4** in terms of the absorption spectrum in addition to the different elution behaviors, as discussed already. Moreover, there is apparent difference between the spectra of $Dy_3N@C_{78}$ and that of $La_2@C_{78}$ (C_{78}:5, D_{3h}) which was characterized very recently.[40]

For **5**, the strong visible absorptions in the range of 400 to 600 nm are found to be quite similar to the case of $Tm_3N@C_{82}$, except that the absorption peaks are more prominent while such an absorption feature is not exhibited by $Sc_2@C_{82}$ (I, II),[42] $Dy_2@C_{82}$ (I),[34] $Er_2@C_{82}$ (I, III),[43] and $Tm_2@C_{82}$ (I, II, III).[43] However, $Dy_3N@C_{84}$ appears more complicated due to the formation of isomers. The absorption spectrum of **8** appears to be like that of $Tm_3N@C_{84}$, except for the larger spectral onset of ∼1485 nm.[29] This implies that the cages of these two analogues might have similar structures but different charge states due to the influence of the metal element on the bonding property of the encaged nitride cluster.[4,30] In addition, **6** shows a completely different absorption feature as evidenced by the NIR absorption at 870 nm, although the spectral onset (∼1514 nm) is close to that of **8**. Instead, such an absorption feature is somewhat similar to those of $Sc_2@C_{84}$ (III, D_{2d})[39] and $Dy_2@C_{84}$ (III),[34] suggesting that the similar electronic structures might be preferred for these three while this argument is to be further confirmed.[44]

The UV−vis−NIR spectrum of **7** looks quite similar to that of $Tm_3N@C_{86}$, except that one of the strongest absorption peaks in the visible region (642 nm) is red-shifted and the spectral onset of ∼1482 nm is larger.[29] Likewise, it may be inferred that the cages of these two clusterfullerenes might have similar structures but different charge states. However, the spectrum of **7** is quite different from those reported dimetallofullerenes based on C_{86} cages, e.g., $Sc_2@C_{86}$ (I, II),[42] $Dy_2@C_{86}$ (I, II),[34] and $Er_2@C_{86}$ (I, II, III),[41] which show strong NIR absorptions between 800 and 1600 nm. This suggests that there are no similarities on the electronic structures between **7** and these known $M_2@C_{86}$ dimetallofullerenes.

Finally, **9** appears to be quite exceptional because of its evident NIR absorptions at 1045 and 1462 nm and the smallest band-gap (0.80 eV), which are not accessible at all for the other $Dy_3N@C_{2n}$ clusterfullerenes illustrated above. Such a feature is similar to those of $Dy_2@C_{88}$ (I, II)[34] and $Er_2@C_{88}$ (I, II, III)[41] to some extent. It is known that, as the fullerene cage becomes larger, the number of structural isomers increases and the molecular symmetry is reduced.[33] As a result, there are 35 IPR satisfying structural isomers for the C_{88} cage and C_{88}: 17 (C_s) is predicted to be the one with the lowest energy followed by C_{88}: 7 (C_2) and C_{88}: 33 (C_2).[33,41,45] Therefore, a tentative assignment for the cage structure of **9** might be either C_s or C_2. Since there is no trimetallic nitride clusterfullerenes based on a C_{88} cage isolated and characterized so far, **9** is distinguished as the largest trimetallic nitride clusterfullerene that is isolated and characterized up to now and the most unique member of the

Dy₃N@C₂ₙ Endohedral Fullerenes

J. Phys. Chem. B, Vol. 109, No. 25, 2005 **12327**
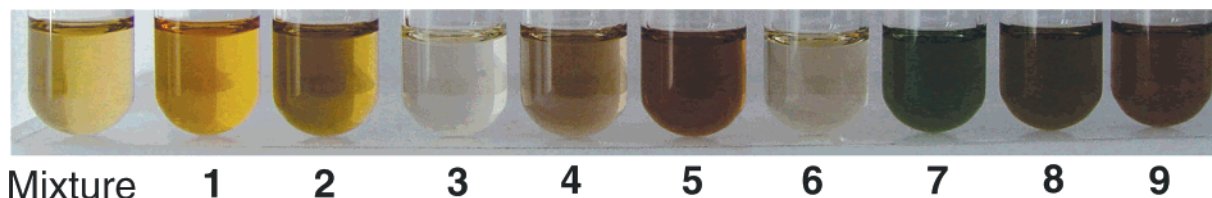
Figure 10. Photographs of a $Dy_3N@C_{2n}$ fullerene extract mixture and clusterfullerenes **1−9** dissolved in toluene.

$Dy_3N@C_{2n}$ clusterfullerene family in terms of its peculiar electronic absorption property.

Based on these different absorption properties, the $Dy_3N@C_{2n}$ clusterfullerenes show a variety of fascinating colors. Figure 10 demonstrates the "colorful" $Dy_3N@C_{2n}$ clusterfullerenes family (**1−9**) dissolved in toluene together with the mixture solution as a reference. Apparently, each clusterfullerene exhibits a unique color, ranging from the unordinary brown-red (**5**), through orange (**1**) and green-yellow (**8**), to the incredible green (**7**) (see Table 2). Such an intriguing feature is seldom demonstrated by the conventional endohedral fullerenes, which are normally yellow after dissolvation in toluene. In fact, like **1**, other $M_3N@C_{80}$ (I) (M = Sc, Tb, Ho, Y, Er, Tm, Gd) clusterfullerenes are also orange based on their specific absorption bands in the visible region.[4,29−31] Except for the above-mentioned cases, the other $Dy_3N@C_{2n}$ clusterfullerenes are generally yellow and the mixture as well.

Conclusion

In summary, for the first time we have successfully produced the $Dy_3N@C_{2n}$ ($38 \leq n \leq 49$) clusterfullerenes, the largest clusterfullerene family explored up to now, at overwhelming yields compared to the empty fullerenes. A series of 10 $Dy_3N@C_{2n}$ clusterfullerenes ($39 \leq n \leq 44$, **1−9**) have been isolated and characterized, including the two isomers for $Dy_3N@C_{78}$ and $Dy_3N@C_{84}$ and three isomers for $Dy_3N@C_{80}$. Compared to the other $M_3N@C_{2n}$ (M = Sc, Tm, Gd) cluster-fullerenes, the $Dy_3N@C_{2n}$ clusterfullerenes appear to be quite unique in terms of the flexibility of the Dy_3N cluster to be encapsulated into the fullerene cage with the largest variability. The optimum production conditions (Dy:C = 1:15, NH_3 pressure = 20 mbar) have been determined and are interpreted in terms of the equilibrium of the chemical reaction between Dy_2O_3 and NH_3. UV−vis−NIR spectroscopic study indicates that the $Dy_3N@C_{2n}$ clusterfullerenes with small cages ($n = 39−41$) are large band-gap (1.38∼1.51 eV) materials, while the band-gaps for those with larger cages ($n = 42−44$) are significantly smaller (0.80∼0.84 eV). The final cage structure assignments for the $Dy_3N@C_{2n}$ clusterfullerenes are under study and will be reported elsewhere.[44] Because of the feasibility of producing the clusterfullerenes with a relatively large Dy_3N cluster encaged in both the C_{80} cage and the larger cages at high yields, the present $Dy_3N@C_{2n}$ family is particularly interesting and quite promising for potential applications such as new contrast agents in magnetic resonance imaging (MRI), which is underway. We believe that this study provides not only important insights for the trimetallic nitride clusterfullerenes but also new avenues for producing new cage structures.

Supporting Information Available: Chromatograms of the mixture fractions (**3+3′**, **4+5**) and all of the isolated products (**1-9**) running on the Buckyclutcher column, UV−vis−NIR spectra of **1−9** showing the spectral onset regions. This material is available free of charge via the Internet at http://pubs.acs.org.

References and Notes

(1) Shinohara, H. *Rep. Prog. Phys.* **2000**, *63*, 843.

(2) Akasaka, T.; Nagase, S. *Endofullerenes: A New Family of Carbon Cluster*; Kluwer Academic Publishers: Dordrecht, 2002.

(3) Yang, S. H. *Trends in Chem. Phys.* **2001**, *9*, 31.

(4) Dunsch, L.; Krause, M.; Noack, J.; Georgi, P. *J. Phys. Chem. Solids* **2004**, *65*, 309.

(5) Wilson, L. J.; Cagle, D. W.; Thrash, T. P.; Kennel, S. J.; Mirzadeh, S.; Alford, J. M.; Ehrhardt, G. J. *Coord. Chem. Rev.* **1999**, *192*, 199.

(6) Yang, S. F. Ph.D. Thesis, Hong Kong University of Science & Technology, Hong Kong, 2003.

(7) Shinohara, H.; Inakuma, M.; Hayashi, N.; Sato, H.; Saito, Y.; Kato, T.; Bandow, S. *J. Phys. Chem.* **1994**, *98*, 8597.

(8) Almeida-Murphy, T.; Pawlik, T.; Weidinger, A.; Höhne, M.; Alcala, R.; Spaeth, J.-M. *Phys. Rev. Lett.* **1996**, *77*, 1075.

(9) Kirbach, U.; Dunsch, L. *Angew. Chem.* **1996**, *108*, 2518.

(10) Wang, C. R.; Kai, T.; Tomiyama, T.; Yoshida, T.; Kobayashi, Y.; Nishibori, E.; Takata, M.; Sakata, M.; Shinohara, H. *Nature* **2000**, *408*, 426.

(11) Dunsch, L.; Bartl, A.; Georgi, P.; Kuran, P. *Synth. Met.* **2001**, *121*, 1113.

(12) Yang, S. F.; Yang, S. H. *J. Phys. Chem. B* **2001**, *105*, 9406.

(13) Yang, S. F.; Fan, L. Z.; Yang, S. H. *J. Phys. Chem. B* **2003**, *107*, 8403.

(14) Yang, S. F.; Fan, L. Z.; Yang, S. H. *J. Phys. Chem. B* **2004**, *108*, 4394.

(15) Stevenson, S.; Rice, G.; Glass, T.; Harich, K.; Cromer, F.; Jordan, M. R.; Craft, J.; Hajdu, E.; Bible, R.; Olmstead, M. M.; Maitra, K.; Fisher, A. J.; Balch, A. L.; Dorn, H. C. *Nature* **1999**, *401*, 55.

(16) Dunsch, L.; Georgi, P.; Ziegs, F.; Zöller, H. German Patent DE 10301722 A1.

(17) Dunsch, L.; Georgi, P.; Krause, M.; Wang, C. R. *Synth. Met.* **2003**, *135*, 761.

(18) Krause, M.; Kuzmany, H.; Georgi, P.; Dunsch, L.; Vietze, K.; Seifert, G. *J. Chem. Phys.* **2001**, *115*, 6596.

(19) Alvarez, L.; Pichler, T.; Georgi, P.; Schwieger, T.; Peisert, H.; Dunsch, L.; Hu, Z.; Knupfer, M.; Fink, J.; Bressler, P.; Mast, M.; Golden, M. S. *Phys. Rev. B* **2002**, *66*, 035107.

(20) Olmstead, M. M.; de Bettencourt-Dias, A.; Duchamp, J. C.; Stevenson, S.; Dorn, H. C.; Balch, A. L. *J. Am. Chem. Soc.* **2000**, *122*, 12220.

(21) Stevenson, S.; Fowler, P. W.; Heine, T.; Duchamp, J. C.; Rice, G.; Glass, T.; Harich, K.; Hajdu, E.; Bible, R.; Dorn, H. C. *Nature* **2000**, *408*, 427.

(22) Olmstead, M. M.; Bettencourt-Dias, A.; Duchamp, J. C.; Stevenson, S.; Marciu, D.; Dorn, H. C.; Balch, A. L. *Angew. Chem., Int. Ed.* **2001**, *40*, 1223.

(23) Stevenson, S.; Lee, H. M.; Olmstead, M. M.; Kozikowski, C.; Stevenson, P.; Balch, A. L. *Chem. Eur. J.* **2002**, *8*, 4528.

(24) Iezzi, E. B.; Duchamp, J. C.; Fletcher, K. R.; Glass, T. E.; Dorn, H. C. *Nano Lett.* **2002**, *2*, 1187.

(25) Feng, L.; Xu, J. X.; Shi, Z. J.; He, X. R.; Gu, Z. N. *Chem. J. Chin. Univ.* **2002**, *23*, 996.

(26) Iezzi, E. B.; Duchamp, J. C.; Harich, K.; Glass, T. E.; Lee, H. M.; Olmstead, M. M.; Balch, A. L. *J. Am. Chem. Soc.* **2002**, *124*, 524.

(27) Lee, H. M.; Olmstead, M. M.; Iezzi, E.; Duchamp, J. C.; Dorn, H. C.; Balch, A. L. *J. Am. Chem. Soc.* **2002**, *124*, 3494.

(28) Iezzi, E. B.; Cromer, F.; Stevenson, P.; Dorn, H. C. *Synth. Met.* **2002**, *128*, 289.

(29) Krause, M.; Wong, J.; Dunsch, L. *Chem. Eur. J.* **2005**, *11*, 706.

(30) Krause, M.; Dunsch, L. *Angew. Chem., Int. Ed.* **2005**, *44*, 1557.

(31) Krause, M.; Dunsch, L. *ChemPhysChem* **2004**, *5*, 1445.

(32) Duchamp, J. C.; Demortier, A.; Fletcher, K. R.; Dorn, D.; Iezzi, E. B.; Glass, T.; Dorn, H. C. *Chem. Phys. Lett.* **2003**, *375*, 655.

(33) Fowler, P. W.; Manolopoulos, D. E. *An Atlas of Fullerenes*; Clarendon Press: Oxford, 1995.

(34) Tagmatarchis, N.; Shinohara, H. *Chem. Mater.* **2000**, *12*, 3222.

(35) Greenwood, N. N.; Earnshaw, A. *Chemistry of the Elements*; Pergamon: Oxford, 1984.

(36) (a) Yang, S. F.; Dunsch, L., in preparation. (b) Yang, S. F.; Dunsch, L. *Chem. Eur. J.*, submitted.

(37) Fuchs, D.; Rietschel, H.; Michel, R. H.; Fischer, A.; Weis, P.; Kappes, M. M. *J. Phys. Chem.* **1996**, *100*, 725.

(38) Lian, Y. F.; Yang, S. F.; Yang, S. H. *J. Phys. Chem. B* **2002**, *106*, 3112.

(39) Inakuma, M.; Yamamoto, E.; Kai, T.; Wang, Ch. R.; Tomiyama, T.; Shinohara, H.; Dennis, T. J. S.; Hulman, M.; Krause, M.; Kuzmany, H. *J. Phys. Chem. B* **2000**, *104*, 5072.

(40) Cao, B. P.; Wakahara, T.; Tsuchiya, T.; Kondo, M.; Maeda, Y.; Rahman, G. M. A.; Akasaka, T.; Kobayashi, K.; Nagase, S.; Yamamoto, K. *J. Am. Chem. Soc.* **2004**, *126*, 9164.

(41) Tagmatarchis, N.; Aslanis, E.; Prassides, K.; Shinohara, H. *Chem. Mater.* **2001**, *13*, 2374.

(42) Wang, Ch. R.; Inakuma, M.; Shinohara, H. *Chem Phys. Lett.* **1999**, *300*, 379.

(43) Kikuchi, K.; Akiyama, K.; Sakaguchi, K.; Kodama, T.; Nishakawa, H.; Ikemoto, I.; Ishigaki, T.; Achiba, Y.; Sueki, K.; Nakahara, H. *Chem. Phys. Lett.* **2000**, *319*, 472.

(44) Krause, M.; Yang, S. F.; Dunsch, L., in preparation.

(45) Sun, G. Y. *Chem. Phys. Lett.* **2003**, *367*, 26.